Evaluation of structural condition using Wavelet transforms

Koichi KUSUNOKI[1], Ahmed Elgamal[2], Masaomi Teshigawara[3] and Joel P. Conte[2]

[1] *Associate Professor, Dept. ofArchitecture,Yokohama National University, Yokohama. Japan*
[2] *Professor, Dept. of Structural Engineering, University of California, San Diego, USA*
[3] *Professor, Dept. of Architecture, Nagoya University, Nagoya, Japan*
Email: kusunoki@ynu.ac.jp

ABSTRACT :

A technique for analysis of dynamic structural response is developed based on the Wavelet Transform Method (WTM). This technique extends an earlier methodology for structures with a predominant fundamental mode, to multi-degree of freedom situations. The structural behavior is evaluated in the form of a performance curve of the predominant response, as a relationship between the equivalent force and equivalent displacement. This curve, scaled by its corresponding mass ratio may be directly compared to a seismic demand curve for the purpose of condition assessment. In this paper, the decomposition procedure of dynamic structural response using the wavelet transform method is presented. Validity of the procedure is illustrated based on an actual dynamic response data from the Vincent Thomas Bridge (VTB) during the 1987 Whittier earthquake, the 1994 Northridge earthquake, and two ambient vibration events in 2004 are studied.

KEYWORDS: Health monitoring, Quick Inspection, Aftershocks, Seismic performance

1. INTRODUCTION

Quick inspection of existing structures soon after a big earthquake is crucial in order to prevent tragedies due to aftershocks. Civil infrastructures such as bridges, public buildings that are supposed to be shelters need to be evaluated to find out the seismic performance during aftershocks. On the other hand, it is also very important to screen out the buildings that still have enough seismic capacity soon after main shock, since a lot of people may refuge from their houses due to fear of collapse even if they have enough capacity. It can help reduce the number of refugees.

Currently buildings have to be investigated one by one by engineers or researchers. For example, 5,068 engineers and 19 days were needed to investigate 46,000 buildings on a damaged area at the Kobe earthquake. Nineteen days were too long and yet the number of investigated buildings was not enough. Moreover, many buildings were judged as “Caution” level, which needs detailed investigation by engineers. “Caution” judgment is a gray zone and it could not take away anxieties from inhabitants. Furthermore, the current quick investigation system presents a dilemma since buildings should be investigated by visual observation of engineers. Thus, judgment varies according to engineers’ experience.

In order to solve the problems mentioned above, authors have been developing the real-time residual seismic capacity evaluation system, which needs only few relatively inexpensive accelerometers. The system calculates the performance and demand curve from a measured acceleration of the basement and of each point of a structure with inexpensive accelerometers, and further estimate the residual seismic capacity of a structure by comparing these curves. To draw the performance curve, the absolute response accelerations and relative response displacement at each point are needed. A certain fixture is generally needed to measure the drift or the relative response displacement to the basement. This fixture can be obstructive for usage or impossible for a long-span bridge. On the contrary, it is easy to measure accelerations with accelerometers. Therefore, displacements are derived from the accelerations by double integral in the system.

The developed system reported in references is, however, only for structures where the first mode is predominant such as low-rise buildings. High-rise buildings and long-span bridges with not negligible higher mode effect, and eccentric buildings, which have three-dimensional response such as torsion, have more than one predominant vibration mode. Therefore, the method proposed in references cannot be applied, since the performance curve for these structures has more than one predominant mode.

On the other hand, the Wavelet Transform Method (WTM) is recently getting attention as one of the powerful time-frequency analysis methods especially in engineering and medical fields. The WTM is a method that decomposes a signal in temporal domain with holding the best relationship between the time increment and frequency increment for the decomposition. The methodology was proposed in 1982 by J. Morlet, oil exploration engineer in France. The WTM satisfies the uncertainty relation with the highest resolution unlike the Window Fourier transform method.

In this paper, the decomposition method with the WTM for the performance curve calculated with the proposed method will be proposed and the validity of the method will be confirmed with numerical simulations and actual monitoring data from the Vincent Thomas Bridge.

2. PERFORMANCE CURVE DECOMPOSITION WITH WAVELET TRANSFORM

2.1. Outline of wavelet transform method

The WTM is a time-frequency analysis method to show the similarity between a signal $f_{(x)}$ and a mother wavelet. The signal of N data points f_0 is decomposed into a signal that has only certain frequency band, g_1, and remaining, f_1, by Eqn. (2.1).

$$f_0 = g_1 + f_1 \tag{2.1}$$

The decomposed signals g_1 and f_1 have *N/2* data points. By repeating the decomposition procedure, the original signal f_0 is decomposed by Eqn. (2.2).

$$f_0 = g_1 + g_2 + g_3 + \cdots g_n + f_n \tag{2.2}$$

The number of decomposition, *n*, is calculated by Eqn. (2.3).

$$n = \log_2 N \tag{2.3}$$

The eventual remaining f_n is a single value. The decomposed components g_i are orthogonal to each other[1).] g_i and f_i are calculated from Eqn. (2.4) and Eqn. (2.5).

$$g_j = \sum_k d_k^{(j)} \psi\left(2^j x - k\right) \tag{2.4}$$

$$f_j = \sum_k c_k^{(j)} \phi\left(2^j x - k\right) \tag{2.5}$$

where; $d_k^{(j)}$ is the sequence to calculate g_i, $c_k^{(j)}$ is the sequence to calculate f_i, $\psi(x)$ is the mother wavelet, and $\phi(x)$ is the scaling function. The B-spline with an order of 4 was applied to the mother wavelet.

As described above, the WTM is a time-frequency analysis method using a mother wavelet as window. The width of the window in temporal domain $2\Delta_{\hat{f}}$ and frequency domain $2\Delta_{f}$ has the uncertainty relation as stated by Eqn. (2.6). The time increment for g_i, $\Delta_{t,i}$, is calculated by Eqn. (2.7) with the time increment Δ_t of an original signal, $f_{(x)}$.Thus, the Nyquist frequency of g_i, $\Delta_{f,i}$, is calculated by Eqn. (2.8) from (Eqn. 2.6). The WTM is one of the most efficient time-frequency analysis methods, since it theoretically satisfies the minimum uncertainty relation.

$$2\Delta_{\hat{f}} \cdot 2\Delta_{f} \geq 2 \tag{2.6}$$

$$\Delta_{t,i} = \Delta_t \times 2^i \tag{2.7}$$

$$\Delta_{f,i} = \frac{1}{2\Delta_t} \times 2^{i-1} \tag{2.8}$$

2.2. Performance curve decomposition with the WTM

If a structure has more than one predominant vibration mode, the response of the structure cannot be estimated as a single-degree-of-freedom system, since the performance curve for the structure has more than one predominant slope, in other words, more than one predominant angular frequency. To overcome the problem with these kinds of structures, a method to decompose a calculated performance curve with the WTM method described in section 2.1 will be proposed in this section.

Recorded acceleration vector $\{{}_M\ddot{x} + \ddot{x}_0\}$ and integrated displacement from them $\{{}_M x\}$ are decomposed as Eqn. (2.9) and Eqn. (2.10) with the WTM.

$$\{{}_M x\} = \left\{ \sum_{i=1}^{N} g_{Disp,i} + f_{Disp,n} \right\} \tag{2.9}$$

$$\{{}_M \ddot{x} + \ddot{x}_0\} = \left\{ \sum_{i=1}^{N} g_{Accel,i} + f_{Accel,n} \right\} \tag{2.10}$$

where, $g_{Disp,i}$ and $g_{Accel,i}$ are components decomposed of rank *i* of the displacement and acceleration, and $f_{Disp,i}$ and $f_{Accel,i}$ are eventual remaining of the displacement and acceleration, respectively.

$f_{Disp,i}$ and $f_{Accel,i}$ are generally error components, since they are single values and their periods are much longer than that of the structure. Thus, $f_{Disp,i}$ and $f_{Accel,i}$ can be ignored. The representative displacement and representative restoring force are decomposed as Eqn. (2.11) and Eqn. (2.12) using Eqn. (2.9) and Eqn. (2.10).

$$\Delta = \sum_r \frac{\sum_i m_i \cdot {}_i g_{disp,r}}{\sum_i m_i} \tag{2.11}$$

$$\ddot{\Delta} = \sum_r \frac{\sum_i m_i \cdot {}_i g_{Accel,r}}{\sum_i m_i} \tag{2.12}$$

Therefore, the representative displacement and representative restoring force for rank *r*, Δ_r and $\ddot{\Delta}_r$, which is a component decomposed by the WFM, are calculated by Eqn. (2.13) and Eqn. (2.14).

$$\Delta_r = \frac{\sum m_i \cdot {}_i g_{disp,r}}{\sum m_i} \tag{2.13}$$

$$\ddot{\Delta}_r = \frac{\sum m_i \cdot {}_i g_{Accel,r}}{\sum m_i} \tag{2.14}$$

As it is obvious from Eqn. (2.13) and Eqn. (2.14), the slope of the relationship between Δ_r and $\ddot{\Delta}_r$ is the square of the predominant angular frequency of rank *r*, ${}_r\omega^2$.

As described in section 2.1, the number of rank decomposed by the WFM depends only on the number of data points, and the frequency range of each rank depends on the number of data points and sampling rate of the original signal. In other words, they are independent of the degree of freedom of the structure. Even if there are two modes in a rank decomposed by the WTM, it is impossible to separate these two modes numerically because of the uncertainty relation.

If no obvious correlation can be seen between Δ_r and $\ddot{\Delta}_r$, there is no predominant vibration mode in the frequency range of rank *r*. The maximum number of modes that the WFM is capable of decomposing, is *n*, which is the number of ranks calculated by Eqn. (2.3).

The equivalent mass of rank *r* ${}_rM$ is defined by Eqn. (2.15). The representative displacement ${}_r\Delta'$ and the representative restoring force $-\left({}_r\ddot{\Delta}' + \ddot{x}_0\right)$ are calculated by Eqn. (2.16) and Eqn. (2.17)with the equivalent mass, respectively.

$${}_rM = \frac{\left(\sum m_i \cdot {}_i g_{disp,r}\right)^2}{\sum m_i \cdot {}_i g_{disp,r}^2} \tag{2.15}$$

$${}_r\Delta' = \frac{M}{{}_rM}\Delta_r \tag{2.16}$$

$$\begin{aligned} {}_rQ &= -M \cdot g_{Accel,r} = -M \cdot \ddot{\Delta}_r \\ &= -{}_rM \cdot \left({}_r\ddot{\Delta}' + \ddot{x}_o\right) \\ \Leftrightarrow {}_r\ddot{\Delta}' + \ddot{x}_0 &= \frac{M}{{}_rM}\ddot{\Delta}_r \end{aligned} \tag{2.17}$$

${}_r\Delta'$ and ${}_r\ddot{\Delta}'$ are calculated from the equation of motion with the predominant angular frequency of rank *r*, ${}_r\omega$ (Eqn. (2.18)).

$${}_r\ddot{\Delta}' + 2 \cdot {}_rh \cdot {}_r\omega \cdot {}_r\dot{\Delta}' + {}_r\omega^2 \cdot {}_r\Delta' = -\ddot{x}_0 \tag{2.18}$$

Therefore, ${}_r\Delta'$ coincides with the values of the response displacement under the input motion of $\ddot{x}_0$ with the damping coefficient of ${}_rh$ and predominant angular frequency of ${}_r\omega$. Thus the comparison between ${}_r\Delta'$

and $-\left({}_r\ddot{\Delta}'+\ddot{x}_0\right)$ (performance curve) and demand curve calculated from the input motion gives the residual seismic capacity of the structure.

3. HEALTH MONITORING OF THE VINCENT THOMAS BRIDGE

The Vincent Thomas Bridge is a cable-suspension bridge crossing the main channel of Los Angeles Harbor. This steel bridge, approximately 1850 meters long, accommodates 4 lanes of traffic and consists of a main span of approximately 457 meters, two suspended side spans of 154 meters each, and a ten-span approach of approximately 545 meters long on each end. The bridge, completed in 1964 and retrofitted after the 1994 Northridge earthquake, was instrumented with 26 accelerometers in 1980. The location of each sensor is shown in Figure 1. The sampling rate of the data was 50Hz.

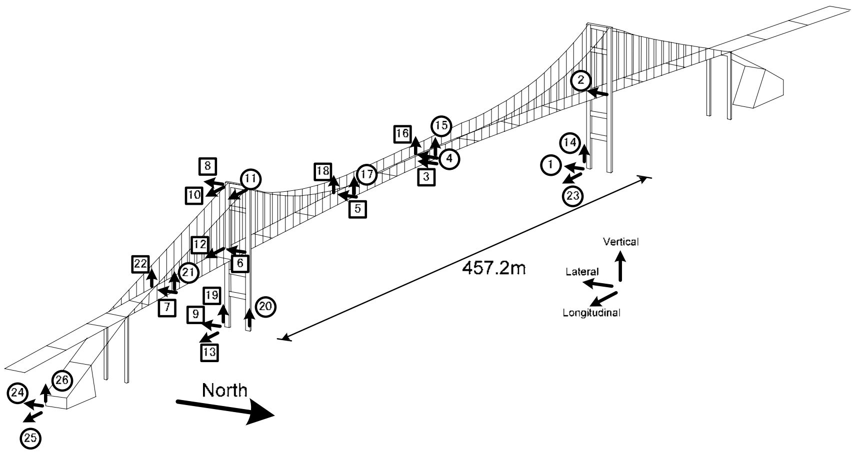

Figure 1 Locations of accelerometer on the Vincent Thomas Bridge

Since this bridge is very long, a lot of modes are supposed to participate in the response. This is the reason why the bridge was used for the study. Moreover, it is also the reason that the monitoring of the bridge started in 1980 and its responses during several earthquakes are available.

When the performance curve was calculated, the response of the bridge was assumed to be axisymmetric at the center of the bridge. The accelerometers used for the study are shown by the symbol □ in Figure 1. The bottom of the east tower was assumed as the only fixed point, then the relative displacements were calculated as the relative values to the channel 9, 13, and 19. The mass ratio for each accelerometer point was assumed by considering the supporting area as 1.0(3)，2.5(5)，2.0(6)，2.0(7)，1.0(8)，1.0(12)，1.0(16)，4.0(18)，3.0(22) (the number in parenthesis indicates the channel number of sensor).

The data recorded during the 1987 Whittier Earthquake and the 1994 Northridge Earthquake were studied. Figure 2 and Figure 3 show the response of channel 10 during the two earthquakes. Furthermore, two data sets recorded during ambient vibrations on November 27th, 2004 were also studied to obtain information on the

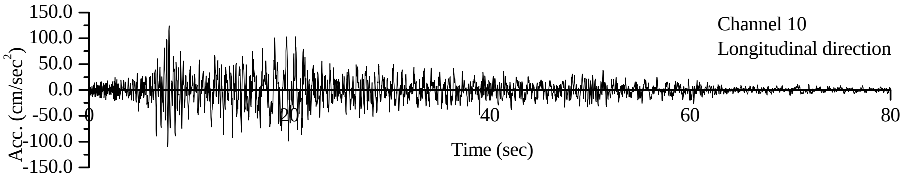

Figure 2 1984 Whittier Earthquake

vibration (9:15AM to 9:30AM) were used in the study. These ambient vibration data were multiplied by the humming window shown in Figure 4 so that the data have 20sec of zero data at both ends. The baselines of the ambient data were also adjusted so that the average value of the data becomes zero. The response of channel 10 during the highest ambient vibration is shown in Figure 5.

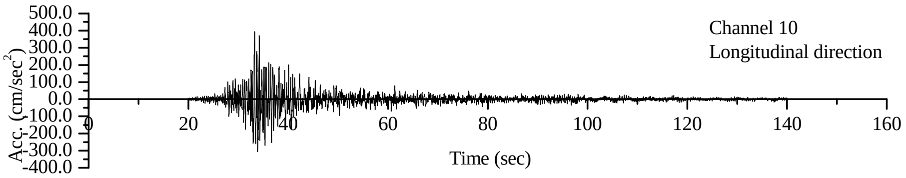

Figure 3 1994 Northridge Earthquake

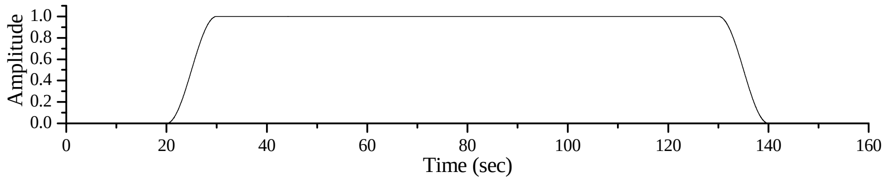

Figure 4 Humming window applied for the monitoring record

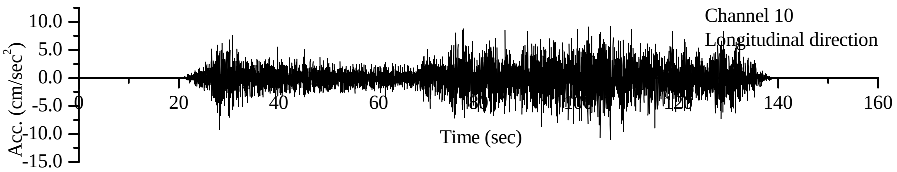

Figure 5 The highest ambient vibration records during November 27th, 2004

Figure 6 shows the performance curve in the longitudinal direction during the Northridge Earthquake. It is obviously difficult to find out some meaningful tendencies in the figure, due to fluctuating from higher mode effects and noise.

Figure 7 shows the time history of the calculated stiffness from decomposed performance curve during the Whittier earthquake. The initial stiffness was 45.15 [1/sec2]. The stiffness degraded down to 28.49 [1/sec2] during the earthquake and ended as 41.03 [1/sec2].

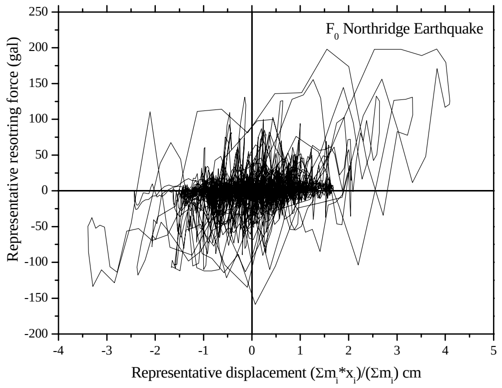

Figure 6 Performance curve in longitudinal direction during the Northridge Earthquake

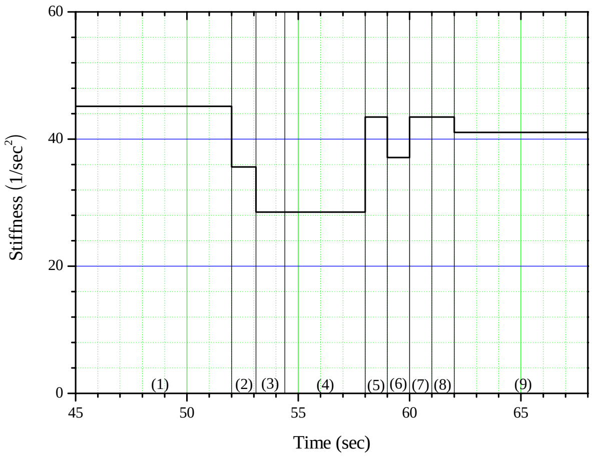

Figure 7 Stiffness degradation during the Whittier Earthquake

Figure 8 shows the responses during the 1994 Northridge Earthquake. Figure 8 (a) shows the accelerations measured at channel 10, 12, and 13. Figure 8 (b) shows the performance curve in the longitudinal direction of the g_{-5} component, which has the Nyquist frequency of 0.781Hz.

Figure 9 shows the time history of the calculated stiffness. The stiffness for portion (1) was 39.44 [1/sec2], little lower than the stiffness at the end of the Whittier Earthquake. The stiffness degraded down to 22.18 [1/sec2] during the earthquake. The stiffness at the end of the earthquake, however, recovered up to 47.72 [1/sec2].

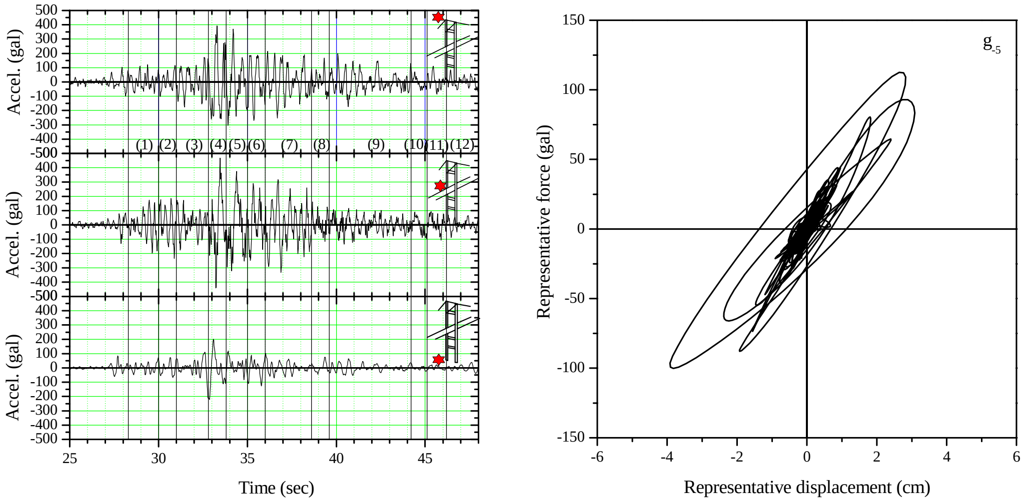

(a) Response acceleration of the tower (b) Performance curve in the longitudinal direction

Figure 8 1994 Northridge Earthquake

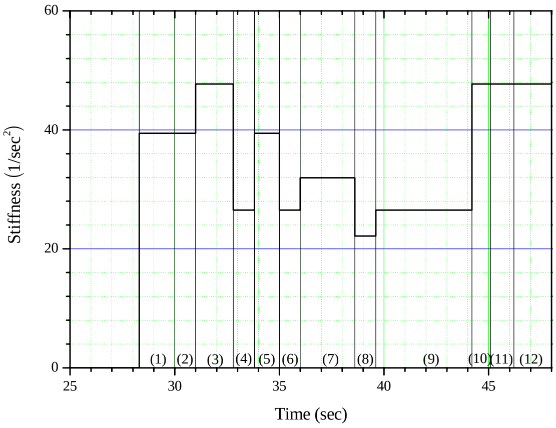

Figure 9 Stiffness degradation during the Northridge Earthquake

Figure 10 (a) and (b) show the envelopes of the performance curve for the lowest ambient vibration from 4:15am to 4:30am on Nov. 27th, 2004 and the highest ambient vibration from 9:15am to 9:30am on the same day. Both figures show that the stiffness was 47.72 [1/sec2], which is exactly the same as the value at the end of the Northridge Earthquake.

4. CONCLUSIONS

A performance curve decomposition method using the Wavelet transform method was proposed to clear off the higher mode effects from a performance curve. The validity of the method was confirmed with the monitoring data of the Vincent Thomas Bridge. Results from the studies are as follows;

- A performance curve decomposition method using Wavelet transform method was proposed.
- The developed WTM can efficiently decompose the dynamic response into its primary response frequency bands.
- In the investigated cases, the predominant performance curves of the VTB in the longitudinal and the vertical directions were successfully extracted.
- A reduction in the longitudinal stiffness of the VTB is documented during the large cycles of dynamic response. Stiffness in the longitudinal direction has not changed due to the imparted earthquake excitations during the last 20 years.

REFERENCES

Susumu SAKAKIBARA (1995). SUURI KAGAKU Wavelet Beginners Guide, Tokyo Denki University Publishing (in Japanese).

Koichi KUSUNOKI and Masaomi Teshigawara (2003). A New Acceleration Integration Method to Develop A Real-Time Residual Seismic Capacity Evaluation System, *Journal of Structural And Construction Engineering*, **No.569**, 119-126 (in Japanese).

Koichi KUSUNOKI and Masaomi TESHIGAWARA (2004). Development of Real-Time Residual Seismic Capacity Evaluation System –Integral Method and Shaking Table Test With Plain Steel Frame-, *13th world conference on earthquake engineering*, **CD-Rom.**

Paul S Addison (2002) . The Illustrated Wavelet Transform Handbook, Institute of Physics publishing.

Building Center of Japan (BCJ) (1996). Report on The Reconnaissance Committee on The Building Damages due to the Hanshin-Awaji Great Earthquake Disaster, 1995 - Summerization - (in Japanese).

Japan Building Research Promotion Association (BRPA) (2007). Guidelines for Performance Evaluation of Reinforced Cconcrete Buildings, Gihodo (in Japanese).

Iwan, W. D., et al.(1985). Some Observations on Strong-motion Earthquake Measurement using a Digital Accelerograph, *Bulletin of the Seismological Society of America*, **Vol. 75**, 1255-1246.

X. He, B. Moaveni, J.P. Conte, A. Elgamal, and S. Masri, (2004). System Identification of Vincent Thomas Bridge using Simulated Wind Response Data, *the Proceedings of the Second International Conference on Bridge Maintenance, Safety and Management (IABMAS'04)*.

A. M. Abdel-Ghaffar, S. F. Masri, and A. –S. M. Niazy (1992). Seismic Performance Evaluation of Suspension Bridges, *Tenth World Conference of Earthquake Engineering*, 4845-4850.

A. M. Abdel-Ghaffar and G. W. Housner (1978). Ambient Vibration Tests of Suspension Bridge, *Journal of the Engineering Mechanics Division*, **EM5**, 983-999.

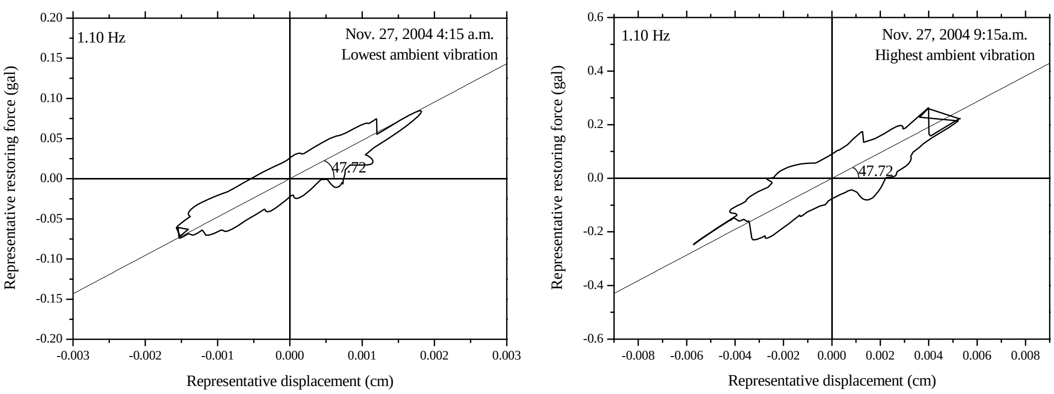

(a) Lowest record (b) Highest record

Figure 10 Envelope curve of performance curve of the lowest ambient vibration